

Formation of microns long thin wire networks with controlled spatial distribution of elements

*Long Pu, Hua Fan, Vivek Maheshwari**

Department of Chemistry, Waterloo Institute for Nanotechnology, University of Waterloo, 200 University Ave. West, Waterloo ON N2L 3G1 Canada.

Materials and Methods

1. Synthesis of Gold Nanoparticle Chains

10 nm citrate capped gold nanoparticle solutions were purchased from BBI solutions (5.7×10^{12} nanoparticles per ml). 500 μl of 5 mg ml^{-1} PtCl_4 was added to a glass vial which contains 3.0 ml of the 10 nm Au nanoparticle solution. Similarly, 150 μl of 2 mg ml^{-1} RuCl_3 was added to assemble 3.0 ml of the Au nanoparticle solution. Metal cations used for the assembly process can vary from monovalent to tetravalent. The variations in cations will lead to different amount and time required for assembly. The difference is expected to be a combined effect of the valency, electronegativity, and hydrodynamic radius of the different cations. For each cation the ideal amount needed for self-assembly is first confirmed by a series of experiments. The cation amount that leads maximum red shift in the plasmon resonance of the Au nanoparticles without destabilizing the suspension is used for self-assembly. The solutions were put on a vortex mixer for assembling of Au-nanoparticles. Assembling time varies from 8 to 24 h for different metal cations. The completion of the assembly was ascertained by UV-Vis measurements when no shift in the plasmon resonance peak was observed

over the course of several hours. By inter-mixing these solutions after the formation of assembled chains at varying stages, spatial control of different cations is achieved. Samples with different Pt:Ru elemental compositions: 100:0 (pure Pt), 95:5, 90:10, and 80:20 were synthesized by varying the volume of each assembled solution in the mixture solution. The final solution is mixed for enough time to allow the assembly of the final structures, in which there are two cations adsorbed onto the Au surface with a spatial distribution. Sodium borohydride (NaBH_4) was then added after the assembly as a reducing agent to the solution for reduction of the metal cations. The amount of NaBH_4 required was calculated based on the valency of the metal cation and 20-30 % in excess of that amount was added. The color of the solution typically changes due to the reduction of the metal ions to the corresponding metal species. For e.g. on reduction of Pt^{4+} -Au solution, the color changes from initial deep blue to grey-black due to formation of Pt metal. Following this the solution was left for at least 2 hrs. before use. The prepared solutions are stable for days and are used as needed.

2. Characterizations

The self-assembled Au nanoparticle chains were characterized by ultraviolet-visible spectroscopy (UV-Vis), and dynamic light scattering (DLS) was used for confirming the size increase in assembled chain-like structures. X-ray photoelectron spectroscopy (XPS) technique was used to characterize the surface composition of the synthesized materials. The crystal structure was characterized by glancing incidence X-ray diffraction (GIXRD) using a PANalytical X'Pert Pro MRD diffractometer with $\text{Cu K}\alpha$ radiation ($\lambda = 1.54 \text{ \AA}$) at an incidence angle of 0.4° . Transmission electron microscopy (TEM) was carried out to examine the morphologies and sizes of the catalysts. Bruker Vertex 70 spectrophotometer was used to record FTIR spectra of the

pristine Au-Ru-Pt chains and also after 2000 cycles. The pellets were prepared by mixing products with potassium bromide, KBr, at a mass ratio of 1:100. The spectrum of the initial Au-Ru-Pt chains was obtained by subtracting the ambient background. While the product that collected after cycling was measured by using the initial AuPt chain as background.

3. Electrochemical Measurements

Electrochemical measurements were carried out using a CompactStat electrochemical interface & impedance analyzer at room temperature. A standard three-electrode set up has been used for all experiments. In all cases, a Ag/AgCl/Saturated KCl electrode was used as the reference electrode, and a Pt wire was used as the counter electrode. A 3 mm (diameter) glassy carbon electrode (GCE) was used as the substrate for depositing the catalyst solutions. Before each measurement, the GCE was polished using 0.05 μm alumina powder. The catalyst solutions were sonicated for 1 h, followed by immediate deposition of 5 μl of the catalyst solution onto the GCE. The working electrodes were then left for 2 h for the evaporation of electrolytes and complete deposition of catalysts.

Prior to all experiments, the GCEs were rinsed with DI water. As the pretreatment step for all samples, conditioning cycles in an acidic solution of 0.1 M HClO_4 for 100 cycles from -0.05 V to 0.6 V with a scan rate of 200 mV/s were done. The electrochemically active surface area measurements were then determined by integrating the hydrogen adsorption charge on the cyclic voltammetry (CV) at room temperature in nitrogen saturated 0.1 M HClO_4 solution with a scan rate of 50 mV/s. Electrooxidation of ethanol was performed in 0.1 M HClO_4 and 1 M ethanol with a scan rate of 50 mV/s. ChronoAmperometry (CA) measurements were performed at a

constant voltage of 0.5 V for 45 min in the same solution, to determine the stability/life-time of the catalysts. For comparison, commercial Pt/C (20 wt. % loading, Sigma-Aldrich) was used as the baseline/control catalyst, and same procedures were conducted for all experiments. CO adsorption was done by keeping the potential at -0.20 V for 20 mins while bubbling CO through the acidic solution of 0.1 M HClO₄. Nitrogen was bubbled again for 10 mins to remove any of the residual CO in the electrolyte. CO stripping was then carried out by doing CV cycles in 0.1 M HClO₄ solution from -0.2 V to 1.2 V at 20 mV/s.

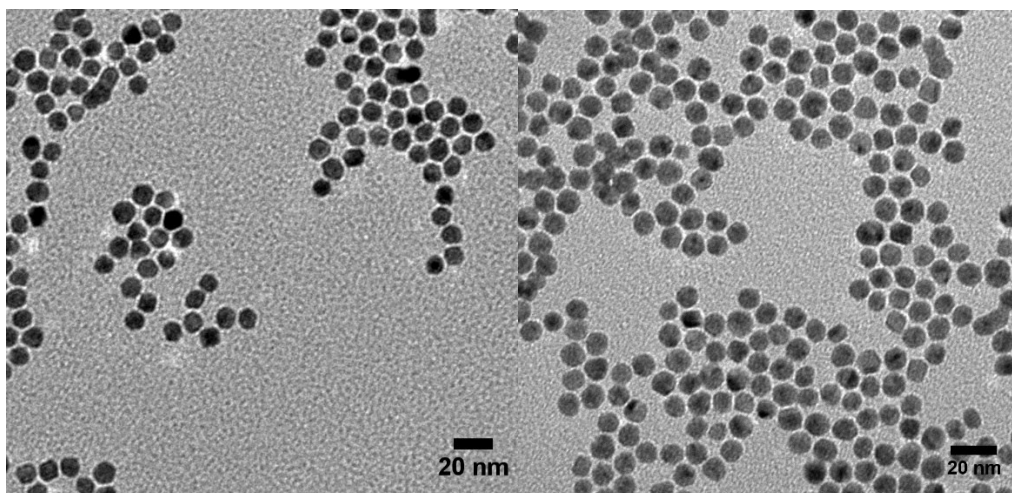


Figure S1. TEM images showing the 2 nm spacing between assembled nanoparticles.

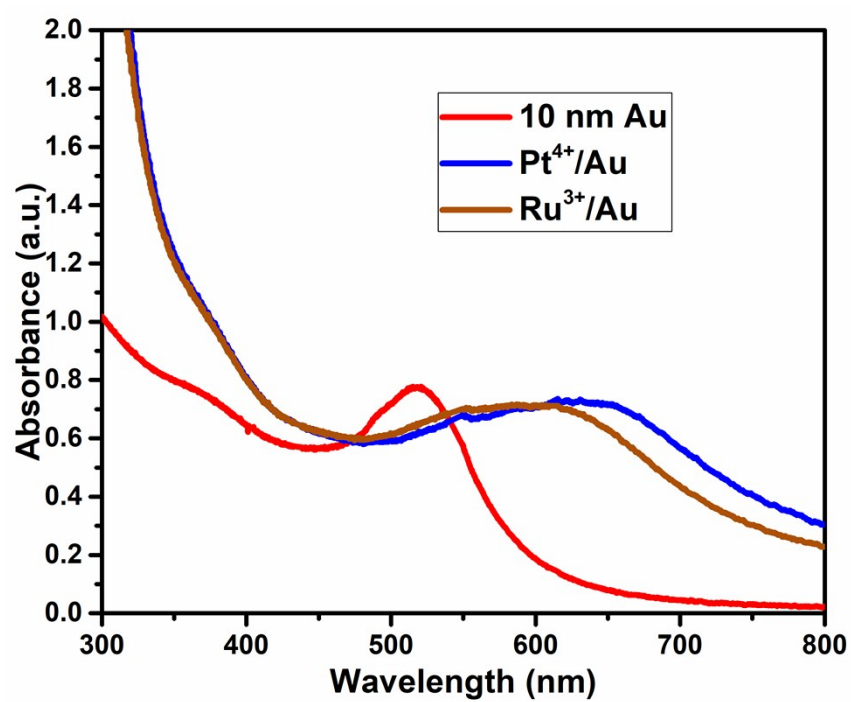


Figure S2. UV-Vis spectrum of metal cations assembled chains.

Table S1. Average size and zeta potential values measured using DLS.

Sample number	Size (nm)	Zeta potential (mV)
1	198.4	-38.5
2	223.8	-37.2
3	226.4	-33.4
4	190.8	-41.0
5	188.6	-33.3
6	245.5	-36.1
7	229.5	-33.6
8	277.7	-34.5
Average	222.6	-35.6

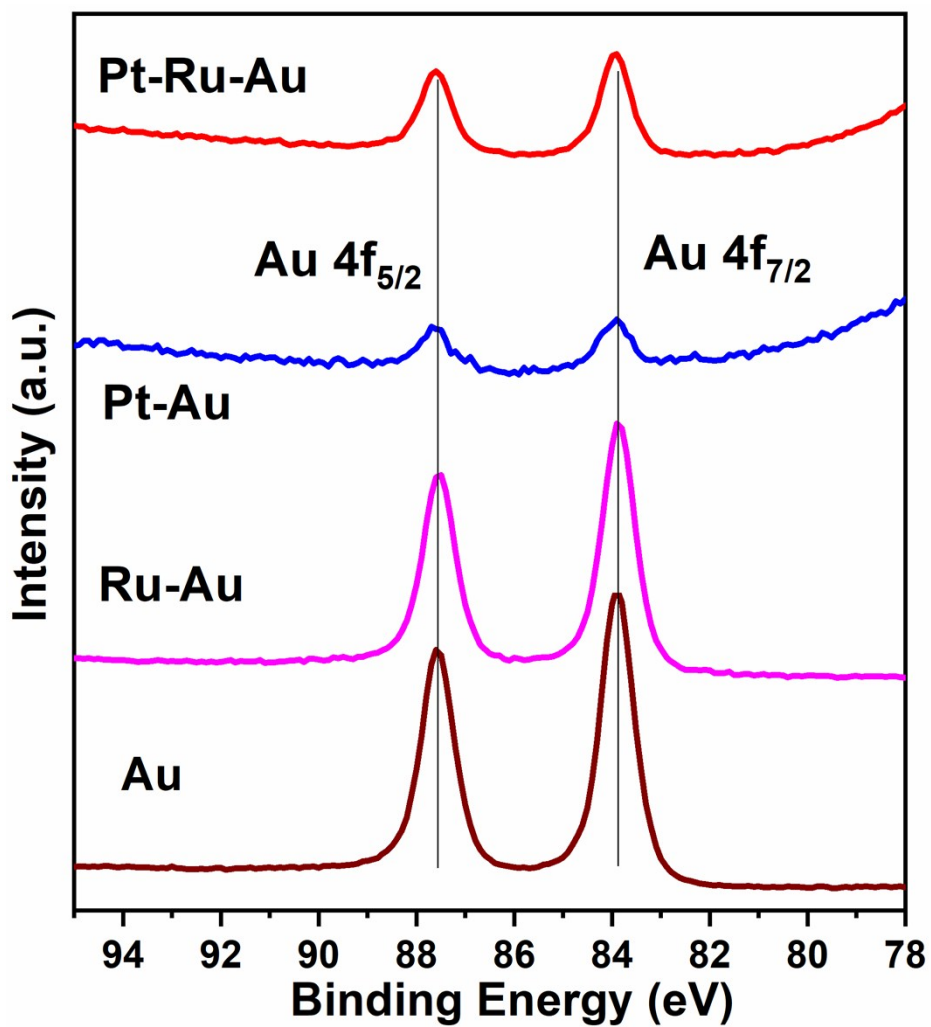


Figure S3. XPS spectra of plain Au nanoparticles, Ru-Au, Pt-Au, and Pt-Ru-Au nanocomposites.

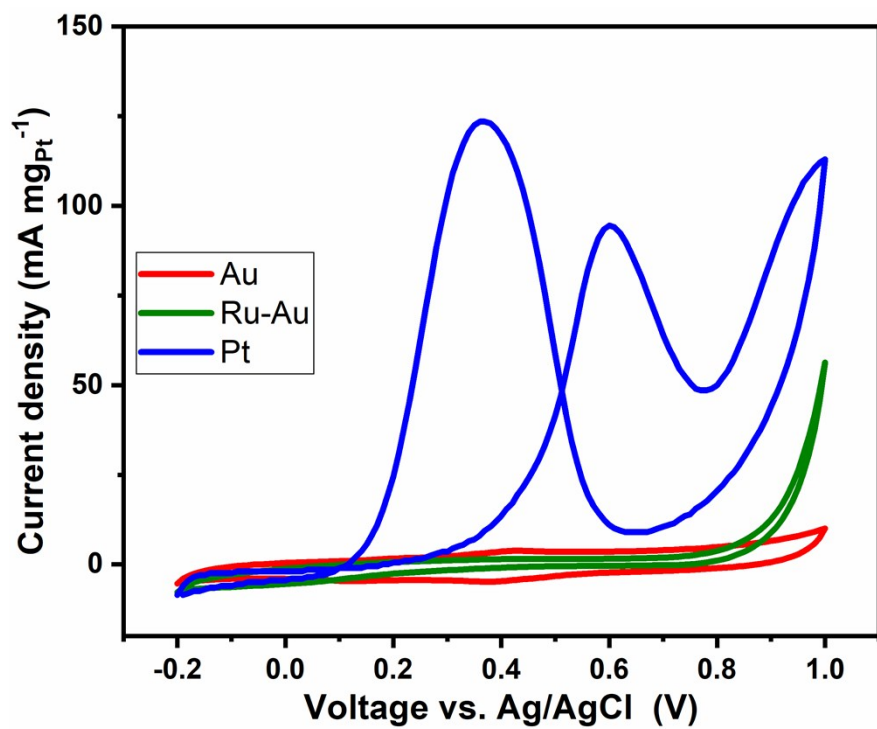


Figure S4. CVs of EOR measurements in 0.1 M HClO₄ and 1 M ethanol at 50 mV s⁻¹ of plain Au nanoparticles, Ru-Au nanocomposite, and reduced Pt⁴⁺ in water without the Au nanoparticle chains.

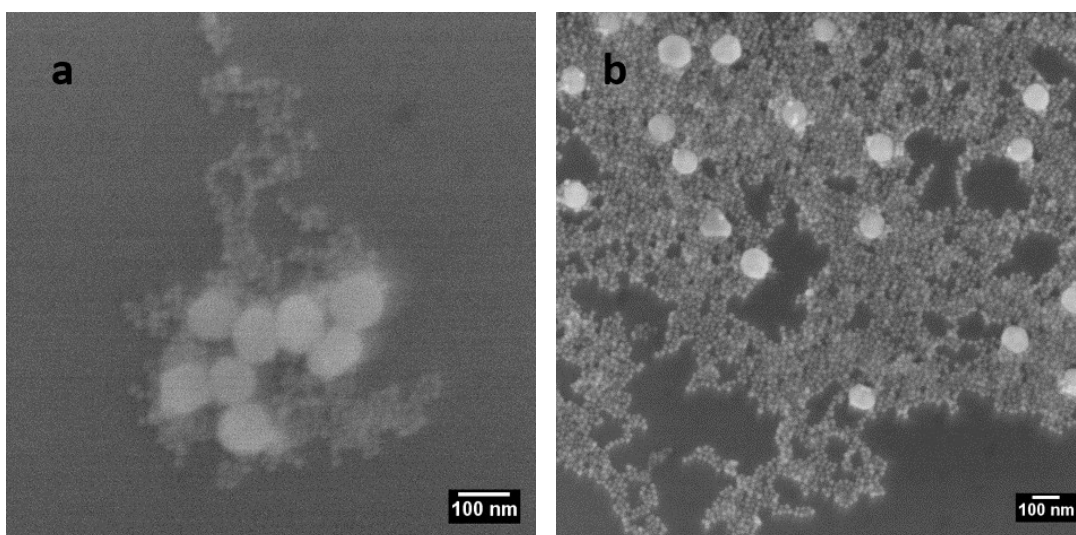


Figure S5. FESEM images of assembled 10 nm and 100 nm Au nanoparticles mixed at different stages: (a) two solutions mixed after self-assembly, (b) mixed at the beginning before the self-assembly.

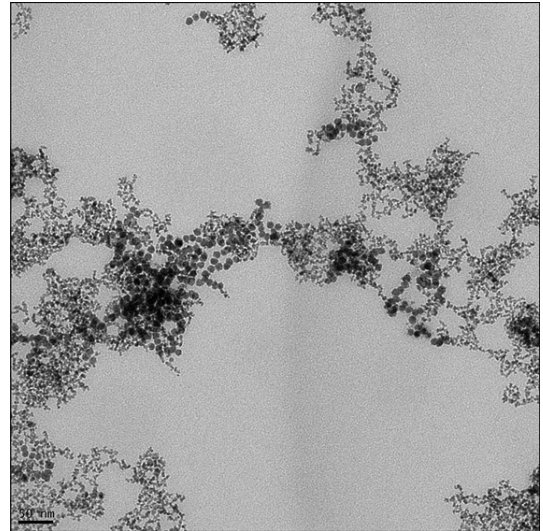
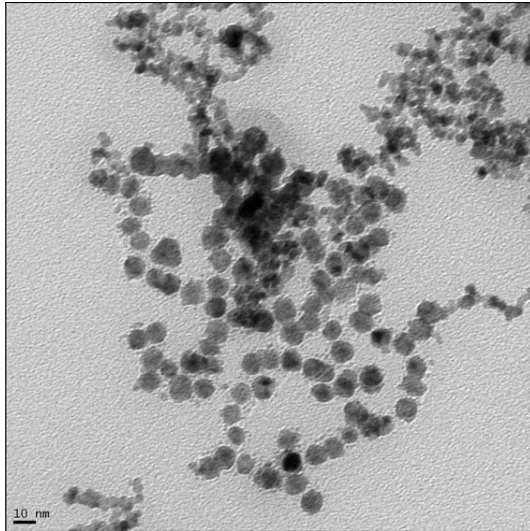
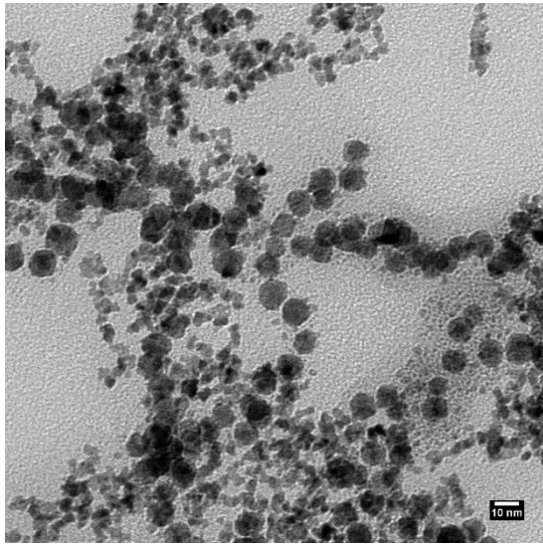
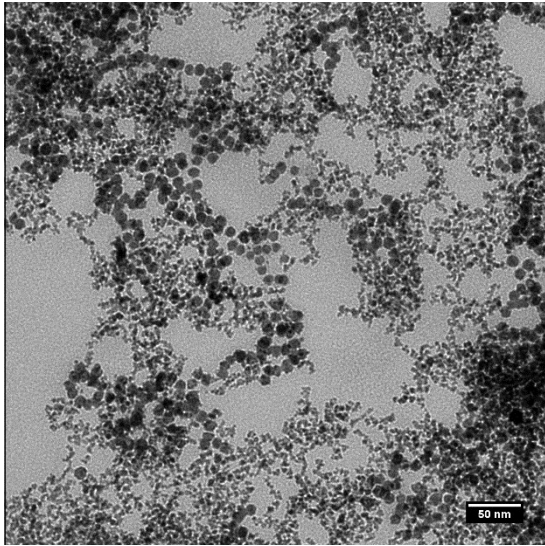


Figure S7. TEM images of Pt-Ru-Au_{end} catalyst at different magnifications. The scale bar in the image on the right is 50 nm.

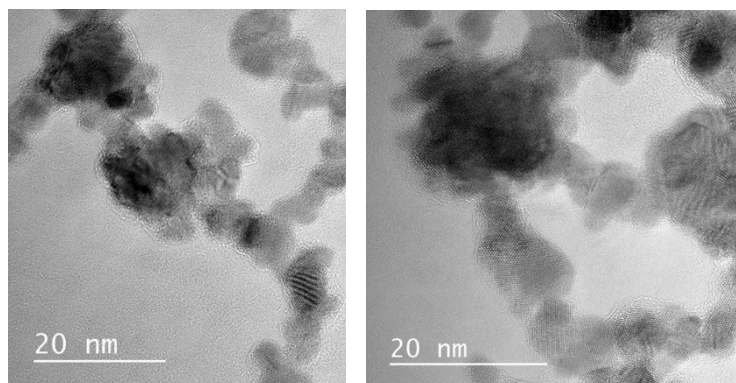


Figure S8.
HRTEM
images of
Pt-Au
catalyst
showing the
formation
of Pt on the
surface of
the Au

nanoparticles and as thin nanowire network.

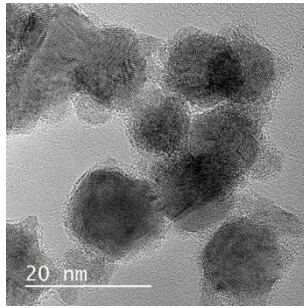
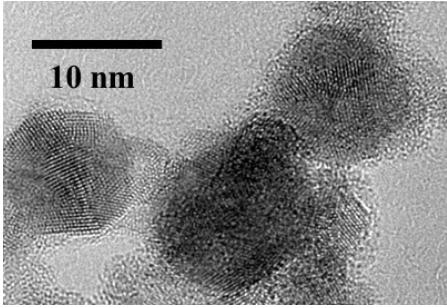


Figure S9. HRTEM images of Ru-Au catalyst showing the formation of a thin layer of Ru on the surface of the Au nanoparticles.

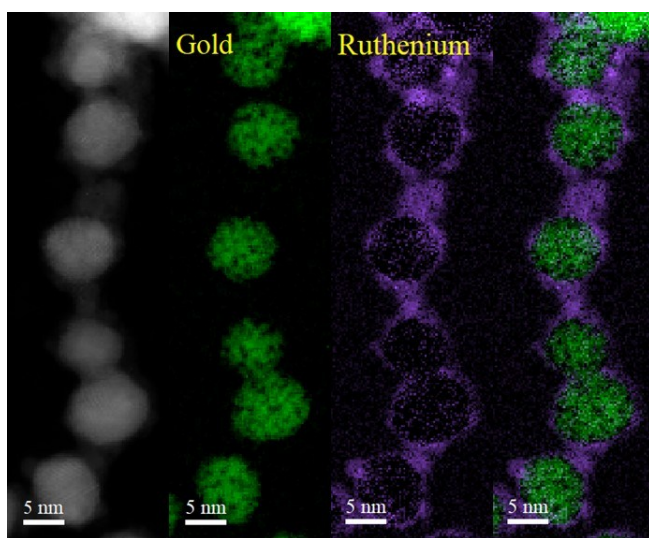


Figure S10. EELS map of Ru-Au catalyst showing elemental distribution, which confirms the formation of a thin layer of Ru on the surface of the Au nanoparticles.

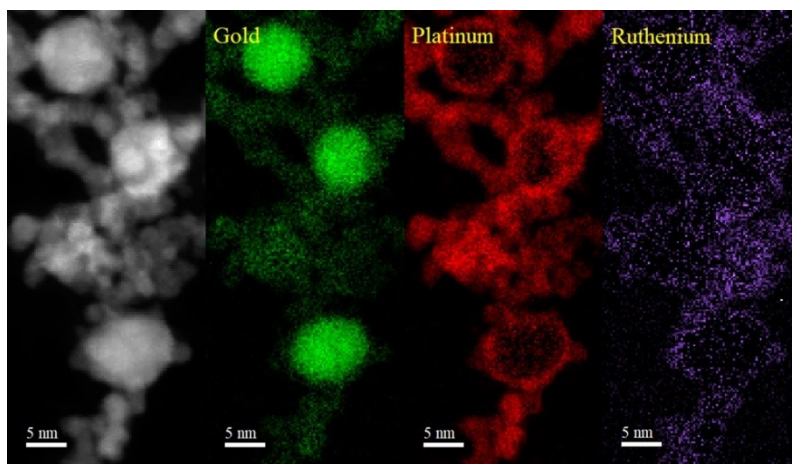


Figure S11. EELS map of Pt-Ru-Au_{beg} catalyst showing the homogenous elemental distribution for Pt and Ru.

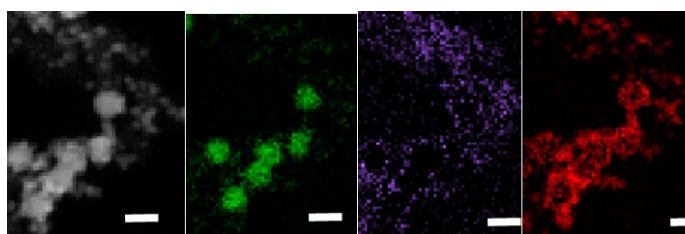


Figure S12. EELS map of Pt-Ru-Au_{end} catalyst showing the distinct domains of the elemental distribution for Pt and Ru. In this image we can see that the Pt domain extends from the middle to the bottom left. While the Ru domain is mostly across the top half from middle to top left.

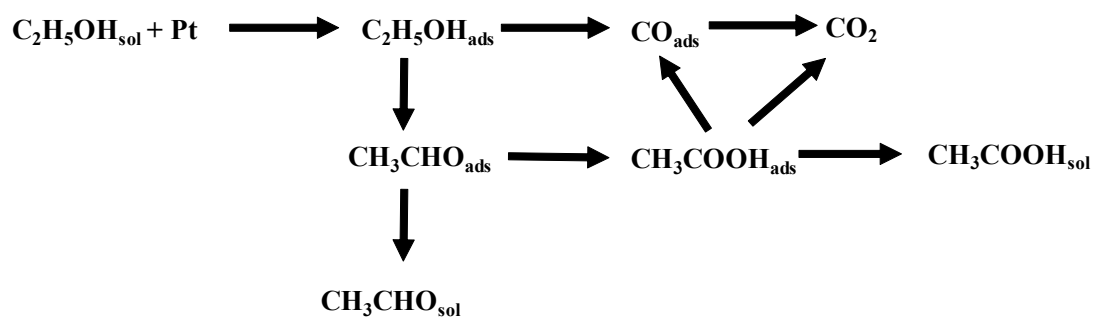


Figure S13. The possible reaction pathways for oxidation of ethanol to CO₂ and other intermediates.¹

References:

1. V. K. Puthiyapura, W. F. Lin, A. E. Russell, D. J. L. Brett, C. Hardacre, *Top. Catal.*, 2018, 61, 240.